

Geodesic motions in extraordinary string geometry

Bogeun Gwak,^{*} Bum-Hoon Lee,[†] and Wonwoo Lee[‡]

*Department of Physics and BK21 Division,
and Center for Quantum Spacetime,
Sogang University, Seoul 121-742, Korea*

Hyeong-Chan Kim[§]

*School of Liberal Arts and Sciences,
Chungju National University, Chungju 380-702, Korea*

Abstract

The geodesic properties of the extraordinary vacuum string solution in (4+1) dimensions are analyzed by using Hamilton-Jacobi method. The geodesic motions show distinct properties from those of the static one. Especially, any freely falling particle can not arrive at the horizon or singularity. There exist stable null circular orbits and bouncing timelike and null geodesics. To get into the horizon or singularity, a particle need to follow a non-geodesic trajectory. We also analyze the orbit precession to show that the precession angle has distinct features for each geometry such as naked singularity, black string, and wormhole.

PACS numbers: 04.70.-s, 04.50.+h, 11.25.Wx, 11.27.+d

^{*}Electronic address: rasenis@sogang.ac.kr

[†]Electronic address: bhl@sogang.ac.kr

[‡]Electronic address: warrior@sogang.ac.kr

[§]Electronic address: hckim@cjnu.ac.kr

I. INTRODUCTION

A well known static vacuum hypercylindrical solution of the Einstein equation in five dimensions is the Schwarzschild blackstring solution, which is characterized by the ADM mass density M and has a horizon with topology $S^2 \times R^1$. The Schwarzschild black string background is known to be unstable under small gravitational perturbations along the fifth direction if the corresponding length is greater than some threshold - the so-called Gregory-Laflamme (GL) instability [1, 2]. The full non-linear evolution of a black string beyond this threshold might result in a black string breaking up into separate black holes or would settle into a stable, static non-uniform black string state [3].

Because of the instability, the hypercylindrical vacuum solutions [4, 5] of the Einstein equation in five dimensions, which has two independent parameters, was reinvestigated by Lee [6] in which the physical implication of the two parameters were correctly interpreted as ADM mass and tension densities [7]. It was also pointed out that the well-known Schwarzschild black string solution corresponds to the case that the tension-to-mass ratio is exactly one half. This implies that the Schwarzschild black string, which was believed to be characterized by the mass density only, is indeed a special case of a wider class of solutions characterized by tension density as well. In Ref. [8] the geometric properties of this class of spacetime with arbitrary tensions were investigated in detail. In Ref. [9] the author studied dyonic brane solutions with tension.

Note also that in 5-dimensional spacetime, there is another class of stationary solutions [10] characterized by the ADM mass and tension densities and momentum along the fifth coordinate. It was shown that the tension density can be made to be the same as the mass density by using the boost symmetry of an asymptotic observer. In that case, the ADM momentum takes its minimum (non-zero) size which we call “momentum charge” in this paper. Therefore, it is impossible to change the “momentum charge” by using the boost transformation of asymptotic observer. Let \mathbf{p} denotes the “momentum charge”-to-mass ratio. As \mathbf{p} increases the metric behaves as a spacetime with a naked singularity, a black string surrounded by an event horizon (or null singularity), or a wormhole. We summarize some of the main properties of the solution in the subsection II A.

Geodesics describing the motion of massive particles or light rays in a given spacetime is one of the best methods to illustrate the geometry of spacetime when the effect of backreaction is negligibly small. In the Schwarzschild spacetime, stable circular orbits for massive particles exist at $r \geq 6G_4M$ only. The orbit at $r = 6G_4M$ is called the marginally stable circular orbit. The circular orbits for $r < 6G_4M$ are unstable. On the other hand, there are no stable circular orbits for photon in the spacetime. The light ray with impact parameter smaller than specific value is captured by the strong gravitational field. The value of critical impact parameter b is $3\sqrt{3}G_4M$ in the Schwarzschild case. The capture cross-section for light rays is $\pi b^2 = 27\pi G_4^2 M^2$, whereas the geometric cross-section is $\pi r_s^2 = 4\pi G_4^2 M^2$ [11]. These are distinguished from Newtonian features of the strong gravitational field. Geodesic motions for a 5-dimensional magnetized Schwarzschild-like solution were studied in Ref. [12], the behavior of a test particle moving in the spacetime is interpreted as a massive magnetic dipole coupled with a massless scalar field. In Ref. [13], the authors studied the geodesic motions of a massive particle and a light ray in the hyperplane orthogonal to the symmetry axis in the 5-dimensional hypercylindrical spacetime [6]. The diffraction angle for bending light and some properties of orbits are analyzed by using analytic and numerical methods. In this paper we investigate how much these features of the geodesics change in the presence

of a “momentum charge”.

In Sec. II, we briefly summarize the stationary metric of the extra-ordinary blackhole and find the geodesic motions by using the Hamilton-Jacobi method. In Sec. III, we study the radial and angular motions of the geodesics by using the effective potential method. Sec. IV is devoted for summary and discussions.

II. GEODESIC MOTIONS IN EXTRA-ORDINARY SOLUTIONS

The most general form of the metric for the spherically symmetric stationary spacetime with a translational symmetry along the fifth spatial coordinate in five dimensions is

$$ds^2 = -F(dt - Xdz)^2 + G[d\rho^2 + \rho^2(d\theta^2 + \sin^2\theta d\phi^2)] + Hdz^2,$$

where F , G , H , and X are functions of the “isotropic” radial coordinate ρ only. Note that the fifth direction is not assumed to be flat in general, *i.e.*, $H \neq 1$. Such a stationary spacetime was considered in Refs. [14, 15]. Time-dependent solution in a separable form were found in Ref. [16]. A class of solutions allowing the z -dependence was also considered in Ref. [17].

The stationary vacuum hypercylindrical solutions of Einstein equation in 5-dimensions are classified by three classes. First is static and is characterized by ADM “mass” and “tension” densities [6]. Second is stationary and is characterized by ADM “mass” and “momentum charge” densities. Third consists of wormhole like solutions. The static solution is well analyzed in Ref. [8] and its geodesic motion was given in Ref. [13]. The third solution was known in Ref. [5]. The authors in Ref. [13] studied the geodesic motions of a massive particle and a light ray in the hyperplane orthogonal to the symmetry axis. The behaviors of the null geodesics were classified into two categories by the values of the tension-to-mass ratio a . The deflection angles are qualitatively similar to those of the black hole for $-1 \leq a \leq 2$ and different for $a < -1$ or $a > 2$. There exists a parameter range in which the singularity is a weakly naked one, $-1 < a < 2$ and a strongly naked one, $a \leq -1$ or $a \geq 2$, in that analysis. For the timelike geodesics, there is a stable circular orbits for $a < -1$. One of the characteristics of the timelike case is that there exists a marginally stable circular orbit for $-1 < a < 2$. The angular momentum and the radius of this marginal orbit were numerically obtained. As a result, the behavior of trajectories has similar properties to that of Schwarzschild black hole if $-1 \leq a \leq 2$. Thus the solution with $-1 \leq a \leq 2$ corresponds to the weakly naked one following the definition of Virbhadra and Ellis [18].

A simplest nontrivial stationary hypercylindrical solution with momentum along the string direction is the boosted Schwarzschild and Kaluza-Klein bubble solutions with compact extra-dimension [15]. It was shown that the momentum parameter governs a global property of the spacetime (so the spacetime is locally indistinguishable to that of the static one) and there remains nontrivial frame dragging effect. The general stationary solution was first given in Ref. [5] and was known in Ref. [10] to be characterized by two parameters, the “mass” and “momentum charge” densities.

A. Summary of the extra-ordinary solution

The “momentum charge” density \mathcal{P} is a new characteristic quantity defined by the minimum value of ADM momenta seen by asymptotic observers. The extra-ordinary string so-

lution is a class of solutions of Einstein equation in 5-dimensions which has a non-vanishing “momentum charge” density in addition to the “mass” density [10]. We define the ratio of the “momentum charge”-to-“mass”,

$$\mathbf{p} \equiv \frac{\mathcal{P}}{M}, \quad (1)$$

where M is the ADM mass density. The metric of the vacuum stationary hypercylindrical solution of Einstein equation in 4+1 dimensions is

$$ds^2 = \left(\frac{1 + K/\rho}{1 - K/\rho} \right)^{-\frac{2}{\sqrt{3}\sqrt{1-3\mathbf{p}^2}}} [-(\omega^t)^2 + (\omega^z)^2] \quad (2)$$

$$+ \left(\frac{1 + K/\rho}{1 - K/\rho} \right)^{\frac{4}{\sqrt{3}(1-3\mathbf{p}^2)}} \left(1 - \frac{K^2}{\rho^2} \right)^2 (d\rho^2 + \rho^2 d\Omega_{(2)}).$$

The time-like 1-form ω^t and the space-like 1-form ω^z are

$$\omega^t = \cos \Upsilon dt - \sin \Upsilon dz, \quad \omega^z = \sin \Upsilon dt + \cos \Upsilon dz, \quad (3)$$

where t and z are Killing coordinates. The argument Υ is a function of radial coordinate ρ given by

$$\Upsilon(\rho) = \frac{\sqrt{3}\mathbf{p}}{\sqrt{1-3\mathbf{p}^2}} \log \frac{1 + K/\rho}{1 - K/\rho}, \quad (4)$$

which monotonically increases from zero to infinity as ρ decreases from infinity to K for positive \mathbf{p} .

The ADM tension along the fifth direction is the same as the mass density and the parameter K is given by

$$K = \frac{G_5 M \sqrt{1-3\mathbf{p}^2}}{\sqrt{3}}. \quad (5)$$

The ADM momentum of this metric is the same as the “momentum charge”. The ADM momentum, P , with respect to a moving observer with velocity v along the z direction satisfies $P/\mathcal{P} = \sqrt{1+4q^2} \geq 1$ where the boost parameter satisfies $\frac{q}{\sqrt{q^2+1/4}} = \frac{2v}{1-v^2}$. The reality of the parameter K restricts the value of \mathbf{p} to $-\frac{1}{\sqrt{3}} \leq \mathbf{p} \leq \frac{1}{\sqrt{3}}$. Note that the metric is invariant under the change $\mathbf{p} \rightarrow -\mathbf{p}$ and $z \rightarrow -z$. Therefore, we restrict ourselves to the case with non-negative \mathbf{p} without loss of generality. Now we summarize some of the main properties of the metric.

- The “momentum charge” density is restricted to the range $|\mathbf{p}| \leq \frac{1}{\sqrt{3}}$.
- There is a curvature singularity at $\rho = K$ unless $|\mathbf{p}| = \sqrt{\frac{5}{27}}$ or $\frac{\sqrt{2}}{3} \leq |\mathbf{p}| \leq \frac{1}{\sqrt{3}}$. The curvature singularity is shown to be naked if $|\mathbf{p}| < \frac{1}{2\sqrt{3}}$ or null if $\frac{1}{2\sqrt{3}} \leq |\mathbf{p}| < \frac{\sqrt{2}}{3}$.
- The $\rho = K$ surface lies at spatial infinity for $\frac{\sqrt{2}}{3} \leq |\mathbf{p}| \leq \frac{1}{\sqrt{3}}$ and at a finite distance else. Especially, the spacetime becomes asymptotically flat as $\rho \rightarrow K$ for $\frac{\sqrt{2}}{3} < |\mathbf{p}| \leq \frac{1}{\sqrt{3}}$.

- The zero “momentum charge” solution is the static solution with $M = \tau$ in Ref. [6].
- The metric for $\frac{\sqrt{2}}{3} \leq |\mathbf{p}| \leq \frac{1}{\sqrt{3}}$ describes a spacetime with a wormhole-like geometry.
- The area of the S^2 sphere decreases to some finite value and then bounces back to infinity as one approaches to the $\rho = K$ surface from infinity.
- On the other hand, the proper length L of a spacelike segment in t - z plane shrinks down to zero as one approaches to the $\rho = K$ surface.
- As a result of the competition of the S^2 area and the segment length, the total area of the segment $S^2 \times L$ of the $\rho = K$ surface turns out to vanishes for $|\mathbf{p}| < \frac{1}{2\sqrt{3}}$, becomes a finite number for $|\mathbf{p}| = \frac{1}{2\sqrt{3}}$, and diverges for $|\mathbf{p}| > \frac{1}{2\sqrt{3}}$.
- There appears an extremely strong velocity frame dragging. As a result, the coordinates t and z exchange their roles as a time and as a space successively whenever the radial coordinate Υ is increased by $\frac{\pi}{2}$. The Killing vectors $(\partial/\partial t)_a$ [$(\partial/\partial z)_a$] is timelike [spacelike] asymptotically. However, as ρ decreases, it successively becomes spacelike [timelike] then timelike [spacelike] and so on. This account for why the peculiar conserved “momentum charge” cannot be gauged away by the motion of an asymptotic observer.

B. Geodesic motion by using Hamilton-Jacobi method

Since we are considering the geodesic motions, we set the zenith angle $\theta = \pi/2$ without loss of generality. The metric has a spherical symmetry and the translational symmetries along z and t . Therefore, we have three Killing vectors $(\partial_t)^a$, $(\partial_z)^a$, and $(\partial_\phi)^a$ and the corresponding conserved quantities the energy E , the momentum along the string direction p_z , and the angular momentum L .

To have the action of a geodesic for a particle, we turn our attention to the Hamilton-Jacobi method, which is useful to obtain the action itself [11]. The classical action, S , is taken to satisfy the relativistic Hamilton-Jacobi equation

$$g^{ab}\partial_a S \partial_b S + m^2 = 0.$$

We renormalize $m = 1$ for timelike geodesics and $m = 0$ for lightlike geodesics, then we have

$$0 = m^2 + \frac{\cos 2\Upsilon \left[-\left(\frac{\partial S}{\partial t}\right)^2 + \left(\frac{\partial S}{\partial z}\right)^2 \right] + 2 \sin 2\Upsilon \frac{\partial S}{\partial t} \frac{\partial S}{\partial z}}{D^{-\frac{2}{\sqrt{3(1-3p^2)}}}} + \frac{\left(\frac{\partial S}{\partial \rho}\right)^2}{G} + \frac{\left(\frac{\partial S}{\partial \theta}\right)^2}{G\rho^2} + \frac{\left(\frac{\partial S}{\partial \phi}\right)^2}{G\rho^2 \sin^2 \theta}, \quad (6)$$

where

$$G = g_{\rho\rho} = \left(1 - \frac{K^2}{\rho^2}\right)^2 \left(\frac{1 + K/\rho}{1 - K/\rho}\right)^{\frac{4}{\sqrt{3(1-3p^2)}}}, \quad D = \frac{1 + K/\rho}{1 - K/\rho}. \quad (7)$$

Since we have three Killing vectors, those symmetries generate three conserved quantities in the sense that S must be a covariant constant under its action: $\mathfrak{L}_k = k^a \partial_a S = \varepsilon$ where k^a is a Killing vector and ε is the corresponding conserved constant. The physical interpretation

of this is that $\partial_a S$ is cotangent to a geodesic and ε is a conserved quantity along that geodesic. Now, the solution can be obtained to be

$$S = -Et + p_z z + L\phi + S_{\frac{\pi}{2}}(\rho), \quad (8)$$

where E , p_z , and L represent the energy, momentum along z direction, and the angular momentum, the subscript $\frac{\pi}{2}$ implies that the zenith angle $\theta = \pi/2$ and the ρ dependent part is

$$S_{\frac{\pi}{2}}(\rho) = \varepsilon \int^\rho d\rho \sqrt{GD \frac{2}{\sqrt{3}(1-3\rho^2)} \cos 2(\alpha + \Upsilon) - \frac{m^2 G}{\varepsilon^2} - \frac{L^2}{\varepsilon^2 \rho^2}}. \quad (9)$$

In this equation we introduce new parameters,

$$\tan \alpha = \frac{p_z}{E}, \quad \varepsilon = \sqrt{p_z^2 + E^2}. \quad (10)$$

The motion of the coordinates t , z , and ϕ can be obtained by using variation of S with respect to E , p_z , and L :

$$t = \int^\rho d\rho \frac{GD \frac{2}{\sqrt{3}\sqrt{1-3\rho^2}} \cos(2\Upsilon + \alpha)}{\sqrt{GD \frac{2}{\sqrt{3}\sqrt{1-3\rho^2}} \cos 2(\Upsilon + \alpha) - \frac{m^2 G}{\varepsilon^2} - \frac{L^2}{\varepsilon^2 \rho^2}}}, \quad (11)$$

$$z = \int^\rho d\rho \frac{GD \frac{2}{\sqrt{3}\sqrt{1-3\rho^2}} \sin(2\Upsilon + \alpha)}{\sqrt{GD \frac{2}{\sqrt{3}\sqrt{1-3\rho^2}} \cos 2(\Upsilon + \alpha) - \frac{m^2 G}{\varepsilon^2} - \frac{L^2}{\varepsilon^2 \rho^2}}}, \quad (12)$$

$$\phi = \frac{L}{\varepsilon} \int^\rho \frac{d\rho}{\rho^2} \frac{1}{\sqrt{GD \frac{2}{\sqrt{3}\sqrt{1-3\rho^2}} \cos 2(\Upsilon + \alpha) - \frac{m^2 G}{\varepsilon^2} - \frac{L^2}{\varepsilon^2 \rho^2}}}. \quad (13)$$

The geodesics are well defined only in the region where the argument of the square root is positive definite.

We introduce a new time coordinate t' and a new space coordinate z' by

$$t' \equiv t \cos \Upsilon + z \sin \Upsilon = \int^\rho d\rho \frac{GD \frac{2}{\sqrt{3}\sqrt{1-3\rho^2}} \cos(\alpha + \Upsilon)}{\sqrt{GD \frac{2}{\sqrt{3}\sqrt{1-3\rho^2}} \cos 2(\Upsilon + \alpha) - \frac{m^2 G}{\varepsilon^2} - \frac{L^2}{\varepsilon^2 \rho^2}}}, \quad (14)$$

$$z' \equiv -t \sin \Upsilon + z \cos \Upsilon = \int^\rho d\rho \frac{GD \frac{2}{\sqrt{3}\sqrt{1-3\rho^2}} \sin(\Upsilon + \alpha)}{\sqrt{GD \frac{2}{\sqrt{3}\sqrt{1-3\rho^2}} \cos 2(\Upsilon + \alpha) - \frac{m^2 G}{\varepsilon^2} - \frac{L^2}{\varepsilon^2 \rho^2}}}.$$

Note that the vector $(\frac{\partial}{\partial t'})^\mu$ is everywhere timelike contrary to $(\frac{\partial}{\partial t})^\mu$ and $t' = t$ asymptotically. By using the time t' , the action can be rewritten as

$$S = \varepsilon [\cos(\Upsilon + \alpha) t' + \sin(\Upsilon + \alpha) z'] + L\theta \quad (15)$$

$$+ \varepsilon \int^{\rho(t')} \frac{dt'}{\cos(\alpha + \Upsilon)} \left[\cos 2(\alpha + \Upsilon) - \frac{m^2}{\varepsilon^2 D \frac{2}{\sqrt{3}\sqrt{1-3\rho^2}}} - \frac{L^2}{\varepsilon^2 G D \frac{2}{\sqrt{3}\sqrt{1-3\rho^2}} \rho^2} \right].$$

How much time will it take if a rocket travels from $K + \epsilon$ to ρ through radial null (non)-geodesic motion? The outgoing velocity of geodesics with respect to the time coordinate t' is evaluated by differentiating Eq. (14). Of all outgoing radial null geodesics at ρ , the maximal velocity is achieved by taking $\alpha = -\Upsilon(\rho)$:

$$v_{\max} = \left(\frac{d\rho}{dt'} \right)_{\max} = \frac{1}{G^{1/2} D \frac{1}{\sqrt{3}\sqrt{1-3p^2}}} = \left(1 - \frac{K}{\rho} \right)^{\frac{\sqrt{3}}{\sqrt{1-3p^2}}-1} \left(1 + \frac{K}{\rho} \right)^{-1-\frac{\sqrt{3}}{\sqrt{1-3p^2}}}.$$

Therefore, we adjust the energy and momentum of the rocket to satisfy $\alpha = -\Upsilon(\rho)$ at a given time. The shortest time for one information traveling from $K + \epsilon$ to ρ becomes

$$\Delta t' = \int_{K+\epsilon}^{\rho} \left(1 - \frac{K}{\rho'} \right)^{1-\frac{\sqrt{3}}{\sqrt{1-3p^2}}} \left(1 + \frac{K}{\rho'} \right)^{1+\frac{\sqrt{3}}{\sqrt{1-3p^2}}} d\rho'. \quad (16)$$

For small ϵ , we get the explicit values:

$$\Delta t' = \begin{cases} \frac{2^{1+\frac{\sqrt{3}}{\sqrt{1-3p^2}}}}{2-\frac{\sqrt{3}}{\sqrt{1-3p^2}}} K \left(\frac{\epsilon}{K} \right)^{2-\frac{\sqrt{3}}{\sqrt{1-3p^2}}} + \text{finite terms}, & \sqrt{1-3p^2} \neq \frac{\sqrt{3}}{2}, \\ -8K \log \left(\frac{\epsilon}{K} \right) + \text{finite terms}, & \sqrt{1-3p^2} = \frac{\sqrt{3}}{2}. \end{cases} \quad (17)$$

In the $\epsilon \rightarrow 0$ limit, this value diverges for $|p| \geq \frac{1}{2\sqrt{3}}$, which signals the presence of an event horizon or a null singularity at $\rho = K$.

III. EFFECTIVE POTENTIAL FOR THE RADIAL MOTIONS

The momentum is given by $p^\rho = \frac{dx^\rho}{d\lambda} = \frac{d\rho}{d\lambda}$ where λ is the affine parameter. The effective potential for the radial motion of a geodesic can be obtained by inserting the conserved quantities E , p_z , and L into the Hamilton-Jacobi equation (6):

$$\left(\frac{d\rho}{d\lambda} \right)^2 = (g^{\rho\rho} p_\rho)^2 = \frac{1}{G^2} \left(\frac{\partial S}{\partial \rho} \right)^2 = -V_{eff}(\rho), \quad (18)$$

where the effective potential for a particle with mass m and three conserved quantities (E, p_z, L) becomes

$$V_{eff}(\rho) = \frac{(1 - K/\rho)^{\frac{2}{\sqrt{3(1-3p^2)}}-2}}{(1 + K/\rho)^{\frac{2}{\sqrt{3(1-3p^2)}}+2}} \left[-\mathcal{E}^2 \cos 2(\alpha + \Upsilon) + m^2 \left(\frac{1 - K/\rho}{1 + K/\rho} \right)^{\frac{2}{\sqrt{3(1-3p^2)}}} + \frac{L^2 (1 - K/\rho)^{\frac{6}{\sqrt{3(1-3p^2)}}-2}}{\rho^2 (1 + K/\rho)^{\frac{6}{\sqrt{3(1-3p^2)}}+2}} \right]. \quad (19)$$

Now let us analyze the effective potential in detail. For comparison, we put the effective potential of a moving particle having two conserved quantities (E, L) in a Schwarzschild black hole spacetime:

$$V_{\text{Schwarzschild}}(r) = m^2 - E^2 - \frac{2m^2 M}{r} + \frac{L^2}{r^2} - \frac{2ML^2}{r^3},$$

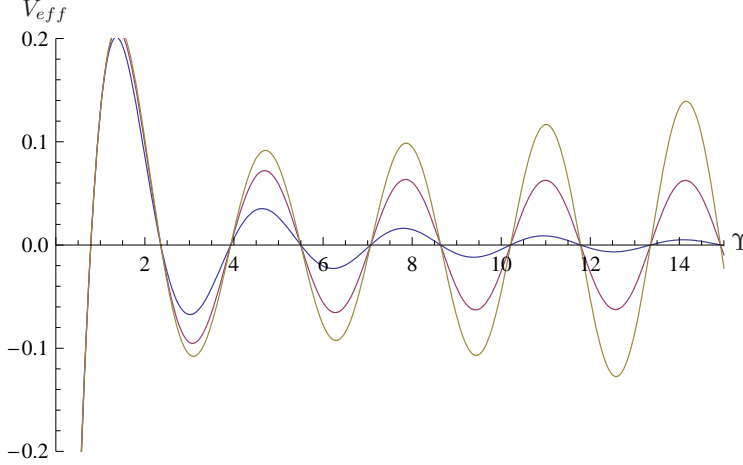


FIG. 1: (color online) Effective potential $V_{eff}(\Upsilon)$ for null radial geodesics. Here, we choose $\mathcal{E} = 1$ and $\alpha = 0$. The blue, purple, and yellow curves correspond to the cases $\mathbf{p} \simeq 0.483$, $\mathbf{p} = \sqrt{2}/3$, and $\mathbf{p} \simeq 0.365$ from the horizontal axis, respectively. For values $\alpha \neq 0$, the roots of the curves move horizontally. The origin corresponds to $\rho \rightarrow \infty$ and the $\Upsilon \rightarrow \infty$ corresponds to $\rho = K$.

where M is the mass of the Schwarzschild black hole and r is the arial radial coordinate. This potential will be negative at $r \rightarrow \infty$ and increases with r because of the mass term $[(1/r)$ potential]. It has a local minimum since the angular momentum gives rise to repulsive force effectively. For smaller angular momentum than $2\sqrt{3}Mm^2$, the local minimum disappears and the potential does not allow any stable (and even unstable) circular geodesic.

Now let us return to the present case. Note that for $\rho \sim K$, the effective potential is dominated by the first term in Eq. (19), which is independent of the mass or angular momentum and oscillates indefinitely around zero. The amplitude of the oscillation is governed by the exponent of $(1 - K/\rho)$,

$$\frac{2}{\sqrt{3(1 - 3\mathbf{p}^2)}} - 2.$$

Therefore, as $\rho \rightarrow K$ the size of V_{eff} decreases to zero if $|\mathbf{p}| > \sqrt{2}/3$, increase to infinity if $|\mathbf{p}| < \sqrt{2}/3$, and approach to a constant value if $|\mathbf{p}| = \sqrt{2}/3$. The oscillatory nature of the effective potential, which comes from the cosine function, is one of the main differences from that of the ordinary static black hole or string solutions with vanishing “momentum charge”. In the case of the Schwarzschild black hole, the energy squared simply determines the height of the effective potential at $\rho \rightarrow \infty$. However, at the present case $E^2 + \mathbf{p}_z^2$ determines the amplitude of oscillation. Because of the oscillation, there appear both the forbidden regions and allowed regions for a particles with given conserved quantities (E, p_z, L) . In the case of a null geodesics with zero angular momentum, the allowed regions are specified to be

$$n\pi - \alpha - \frac{\pi}{4} \leq \Upsilon \leq n\pi - \alpha + \frac{\pi}{4}.$$

The asymptotic region will be allowed here if $-\frac{\pi}{4} \leq \alpha \leq \frac{\pi}{4}$ or $\frac{3\pi}{4} \leq \alpha \leq \frac{5\pi}{4}$ and only the first region is relevant when we restrict ourselves to the particles with positive energy, satisfying $E \geq |p_z|$. Noting this, we may write the allowed region including the asymptotic

in terms of the radial coordinate ρ ,

$$\rho \geq \rho_{\text{boundary}}, \quad (20)$$

$$\coth \left[\frac{\sqrt{1-3\mathbf{p}^2}}{2\sqrt{3}\mathbf{p}} \left(n\pi - \alpha + \frac{\pi}{4} \right) \right] \leq \frac{\rho}{K} \leq \coth \left[\frac{\sqrt{1-3\mathbf{p}^2}}{2\sqrt{3}\mathbf{p}} \left(n\pi - \alpha - \frac{\pi}{4} \right) \right],$$

where n is any positive integer and the outermost boundary of the allowed region ρ_{boundary} is

$$\rho_{\text{boundary}}(\alpha, L=0, m=0) = \coth \left[\frac{\sqrt{1-3\mathbf{p}^2}}{2\sqrt{3}\mathbf{p}} \left(\frac{\pi}{4} - \alpha \right) \right]. \quad (21)$$

For small value of momentum charge-to-mass ratio, $\mathbf{p} \ll 1$, the boundary approaches to K and essentially the boundary becomes the $\rho = K$ surface at $\mathbf{p} = 0$. For $\mathbf{p} \sim 1/\sqrt{3}$ the position of the boundary becomes large $\rho_{\text{boundary}} \rightarrow \infty$. In general, the explicit value of $\rho_{\text{boundary}}(\alpha, L, m)$ will be dependent on L and m explicitly. We compare the radial geodesic motion for $\rho > \rho_{\text{boundary}}$ with that of the Schwarzschild black hole outside of the angular momentum barrier. We show that the properties of the barrier are quite different from that of the Schwarzschild in the following senses,

- Any geodesics cannot go over the potential barrier however high energy the particle has. This fact is denoted by the presence of ρ_{boundary} for any values of E , L , and p_z .
- There exists the boundary ρ_{boundary} for null geodesics even in the absence of an angular momentum barrier. Therefore, the origin of this barrier is not due to the angular momentum but due to the ‘‘momentum charge’’.
- The position of the boundary is crucially dependent on the momentum-to-energy ratio $p_z/E = \tan \alpha$ of the particle rather than the energy itself.

The asymptotic region is not included in the allowed region if $\frac{\pi}{4} < \alpha < \frac{3\pi}{4}$ or $\frac{5\pi}{4} < \alpha < \frac{7\pi}{4}$, where $|p_z| > E$. The allowed region in terms of the radial coordinate ρ in this case is given by the second line of Eq. (20). Note that all allowed regions are compact in ρ and there is no asymptotic region. Note also that the coordinate t is not a time in these regions. Rather, the coordinate z does the role of time, therefore we may understand the condition $|p_z| > E$.

For large ρ , the effective potential takes the form:

$$V_{\text{eff}}(\rho) \sim -E^2 + p_z^2 + m^2 - \frac{2m^2 + p_z^2 - E^2 - 6\mathbf{p}p_zE}{3} \frac{4G_5M}{\rho} \quad (22)$$

$$+ \left\{ \frac{L^2}{G_5^2 M^2 (\frac{1}{3} - \mathbf{p}^2)} - 6 \left(\mathbf{p}^2 - \frac{19}{9} \right) m^2 - 2\mathcal{E}^2 \left[\left(\frac{7}{3} - 15\mathbf{p}^2 \right) \cos 2\alpha + 8\mathbf{p} \sin 2\alpha \right] \right\} \frac{G_5^2 M^2}{3\rho^2}.$$

Observing the zeroth order term, the region $\rho \rightarrow \infty$ is allowed to particles with $E^2 \geq p_z^2 + m^2$. The condition is related to the value of momentum along the extra direction, contrary to the case of the Schwarzschild.

Seeing the $O(1/\rho)$ term, the potential increases with ρ if

$$0 \leq E < -3\mathbf{p}p_z + \sqrt{(9\mathbf{p}^2 + 1)p_z^2 + 2m^2},$$

where we set the lower bound of E to zero since we deal with the situation around $\rho \rightarrow \infty$. We summarize various properties of the effective potential:

- In the absence of “momentum charge” ($\mathbf{p} = 0$), the asymptotic form of the effective potential increases with ρ if $p_{\perp} < m$, where $p_{\perp} = \sqrt{E^2 - p_z^2 - m^2}$ is the momentum along the 3-dimensional space other than the extra-dimension. For particles with high momentum, $p_{\perp} > m$, the effective potential may decrease as ρ increases, which behavior does not happen for the Schwarzschild geometry. In the case of a null geodesics ($m = 0$), the effective potential decreases with ρ .
- For null geodesics moving along the opposite direction to the dragging ($\mathbf{p}p_z < 0$), the asymptotic form of the effective potential increases with ρ if $p_{\perp} < -3\sqrt{2}\mathbf{p}p_z(1 + \sqrt{1 + 1/(9\mathbf{p}^2)})^{1/2}$. This implies that there exist a stable circular orbit for a light at some $\rho > \rho_{\text{boundary}}$, which is completely different from the cases of $\mathbf{p} = 0$ and the Schwarzschild black hole. Some example of this behavior are shown in the next section. For other cases except for this, the effective potential decreases asymptotically for the null geodesics.
- For timelike geodesics, the asymptotic form of the effective potential can decrease or increase according to the parameter. When it decreases asymptotically, the effective potential does not have any local minimum in the outside ($\rho > \rho_{\text{boundary}}$) of the classically forbidden region.

IV. THE GEODESIC MOTIONS

In the present section, we explore the geodesic motions of a massive particle and a light ray under the influence of the effective potential (19) in the extraordinary string geometry. The geodesic motions of a massive particle and the effective potentials for the corresponding motions in the plane at $\theta = \pi/2$ are shown in Figs. 2-11. The corresponding parameter values are written in each figure. We set $m = 1$ for timelike geodesics. In this work, we divide the timelike geodesics into two groups. The first group represents the geodesics with non-zero momentum along the z -direction. The second group represents the geodesics with zero momentum along the z -direction. If we take the geometry with non-zero momentum along the z -direction, each figure shows that the curves are projected on the X - Y plane. The particles move in three different geometries. The first geometry has the naked singularity. The second one corresponds to the black string geometry. The third one corresponds to the wormhole geometry. In the analysis of the geodesic motions, one can usually read off the behaviors of the motions from the shape of the effective potential. However, we visualize the trajectories in detail to show the unusual features such as bouncing off the potential barrier at strong gravitational regime. The particle resides only in the regions of $V_{eff} \leq 0$. In these figures, the radial coordinate ρ is measured in unit of K . For every trajectories, the potential barriers surrounding the geometry exist always as is shown in each figure. If V_{eff} has a local minimum or maximum with $V_{eff} = 0$, there exists the circular motion of a massive particle at that radius. In our cases, there exist stable circular orbits at certain parameter values in each geometry. If V_{eff} has the region of $V_{eff} < 0$, there exist elliptic motions. The trajectories are bounded between perihelion and aphelion points. The second figure in Fig. 2, the third figure in Fig. 3, the first and the fourth figure in Fig. 4, and the third figure in Fig. 7 reveal an unusual behavior showing the motion of a particle bouncing off the potential barrier. This behavior is qualitatively different from that of the spacetime without the “momentum charge”. The first figure in Fig. 2, the third figure in Fig. 3, the

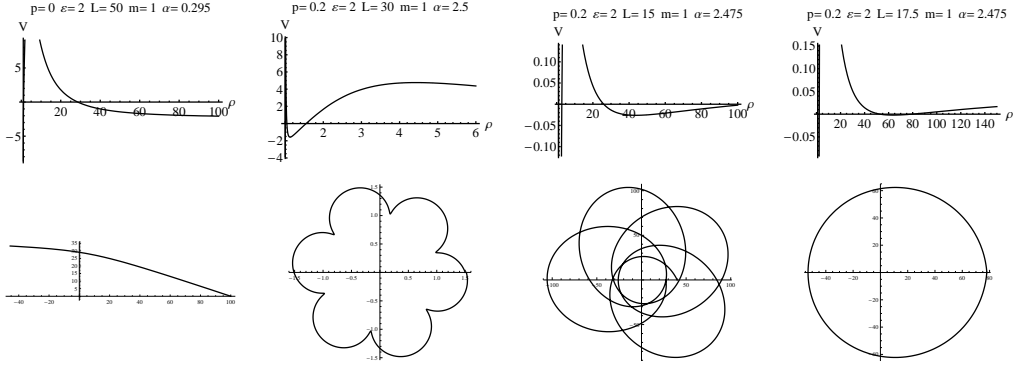


FIG. 2: The effective potential and timelike geodesic orbits in naked singularity spacetime with non-zero momentum along the z -direction. The orbits are plotted in terms of coordinates $x = \rho \cos \phi$ and $y = \rho \sin \phi$. If we take the geometry with non-zero momentum along the z -direction, each figure shows that the curves are projected on the x - y plane. The explicit values of momentum charge \mathfrak{p} of the geometry and the energy E , angular momentum L , and momentum to energy ratio α of particle are given in the figures.

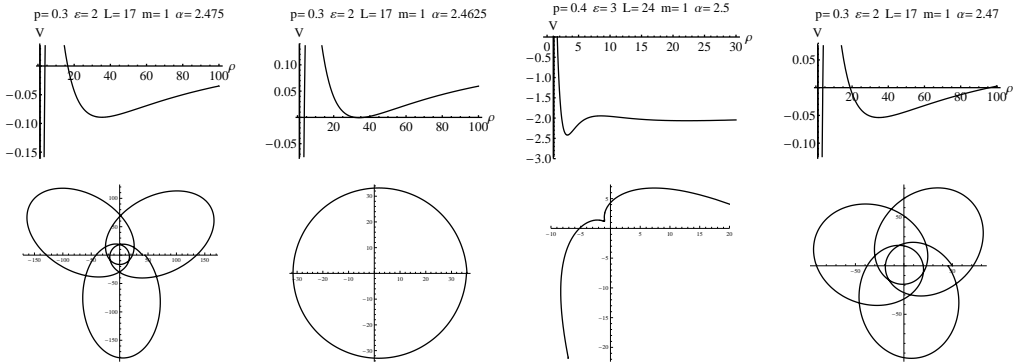


FIG. 3: The effective potential and timelike geodesic orbits in black string spacetime with non-zero momentum along the z -direction.

first figure in Fig. 4, the second figure in Fig. 5, and the third figure in Fig. 6 indicate the hyperbolic motions.

Now, we study the lightlike geodesics ($m = 0$) for non-zero momentum along the z -direction. There exist a stable circular motion (spiral motion if one include the motion along z), the elliptic motion, the hyperbolic motion, and the unusual behavior corresponding to the motion of a particle bouncing off the potential barrier. There are no stable circular orbits for light rays in the Schwarzschild case. The lightlike geodesic motion can be used to understand the gravitational lensing effect. The lensing is described by its deflection angle. In Schwarzschild case, the effective deflection angle of relativistic image is an important clue for getting information of strong gravitational lensing [19].

Next, we consider the massive particle bounded in an orbit around the string solution. At perihelion and aphelion points, ρ reaches its minimum and maximum values ρ_{min} and ρ_{max} , where $d\rho/d\phi$ vanishes. The change in ϕ as ρ decreases from ρ_{max} to ρ_{min} is the same as the

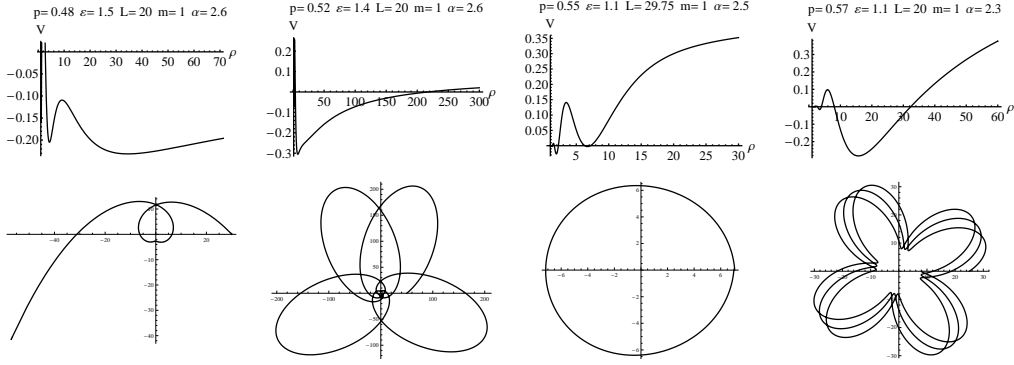


FIG. 4: The effective potential and timelike geodesic orbits in wormhole geometry with non-zero momentum along the z -direction.

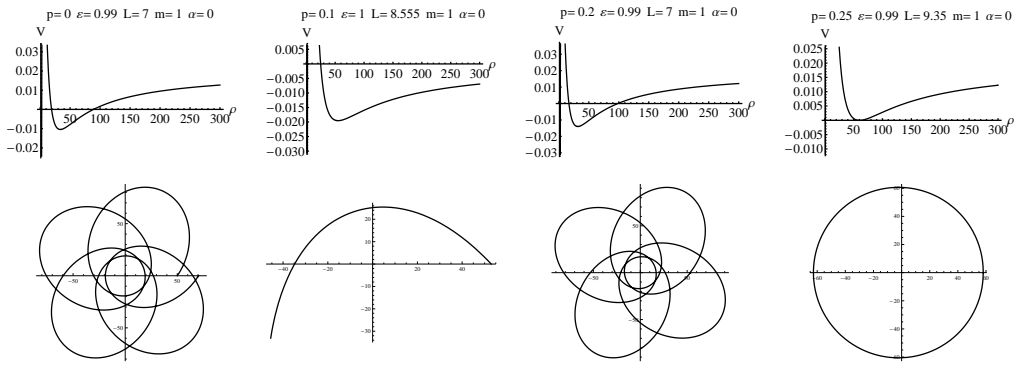


FIG. 5: The effective potential and timelike geodesic orbits in naked singular spacetime with zero momentum along the z -direction.

change in ϕ as ρ increases, so the total change in ϕ per revolution is $2[\phi(\rho_{max}) - \phi(\rho_{min})]$. This is equal to 2π if the orbit was a closed ellipse. Thus, the orbit precession angle is given by

$$\Delta \phi = 2\{[\phi(\rho_{max}) - \phi(\rho_{min})] - \pi\}, \quad (23)$$

where $\phi(\rho_{max}) - \phi(\rho_{min})$ is determined by Eq. (10). If the orbit should precess in the same direction as the motion of the particle, the rate has positive value. In Fig. 11 the curves represent the change of the precession rate versus the values of L , where $m = 1$, $\mathcal{E} = 1$ and $\alpha = 0.1$. The ratio of the momentum charge-to-mass \mathbf{p} changes the precession rate. The rate $\Delta\phi$ is -2π at $L = 0$. This means that $\phi(\rho_{max}) - \phi(\rho_{min}) = 0$ in the present geometry. The numerical results show that the precession rate can be classified into three groups in the range of \mathbf{p} . The first group has the range from 0 to about $0.3 \simeq 1/(2\sqrt{3})$, where $1/(2\sqrt{3})$ denotes the boundary of the naked singularity and black string. In this group, the curve has a peak. There is the highest peak about $\mathbf{p} = 0.15$. And then the magnitude of the peak is decreased as \mathbf{p} increases. The position of the peak is moved to the left as \mathbf{p} increases. The second group has the range from 0.3 to 0.45. The numerical results show that the curves have the tendency to converge to -2π as the value of \mathbf{p} increases. Interestingly, the peak

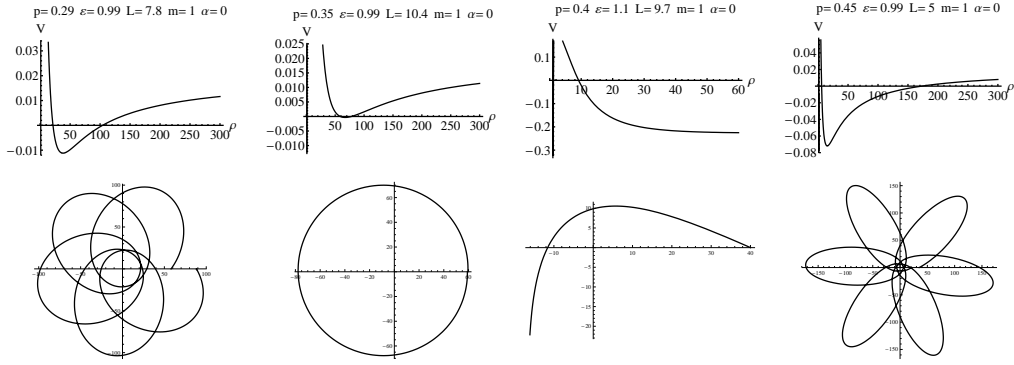


FIG. 6: The effective potential and timelike geodesic orbits black string spacetime with zero momentum along the z -direction.

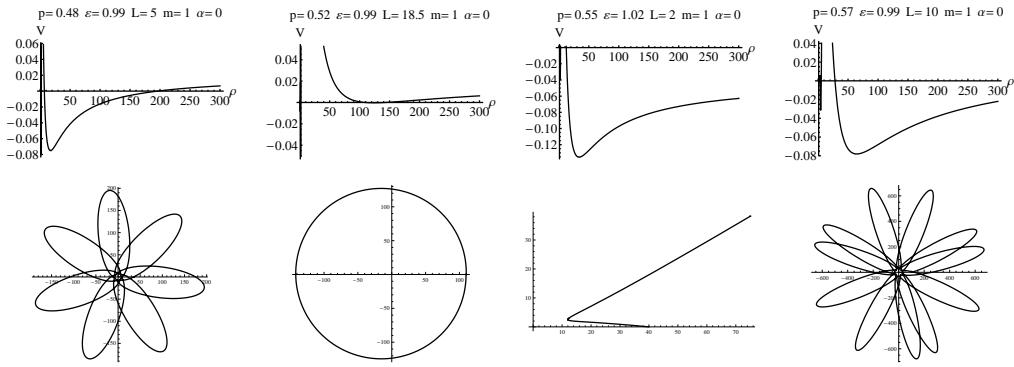


FIG. 7: The effective potential and timelike geodesic orbits in wormhole geometry with zero momentum along the z -direction.

is moved to the right and gone away as \mathbf{p} increases. As the angular momentum increases, there is a tendency to have a circular motion so that the precession angle $\Delta\phi = 0$. The third group has the ranges bigger than 0.5, for that curves the maximum has gone away and it continually increases to zero with angular momentum. Note that the boundary $\mathbf{p} = \sqrt{2}/3$ between the black string and wormhole lies between the two values 0.45 and 0.5. Noting these results, we can distinguish the properties of the geometry by analyzing the angular momentum dependence of the precession angle.

V. SUMMARY AND DISCUSSIONS

We studied the geodesic motions in extraordinary string solutions in 4+1 dimensions. First we show that the extraordinary solution developed in Ref. [10] is classified by the mass and “momentum charge” densities. Central properties of the solution were summarized. Especially, the “momentum charge”-to-mass ratio is restricted to $|\mathbf{p}| \leq 1/\sqrt{3}$. Its geometry takes the form of a naked singularity, a black string with a null singularity, and a wormhole according to the value of $|\mathbf{p}|$.

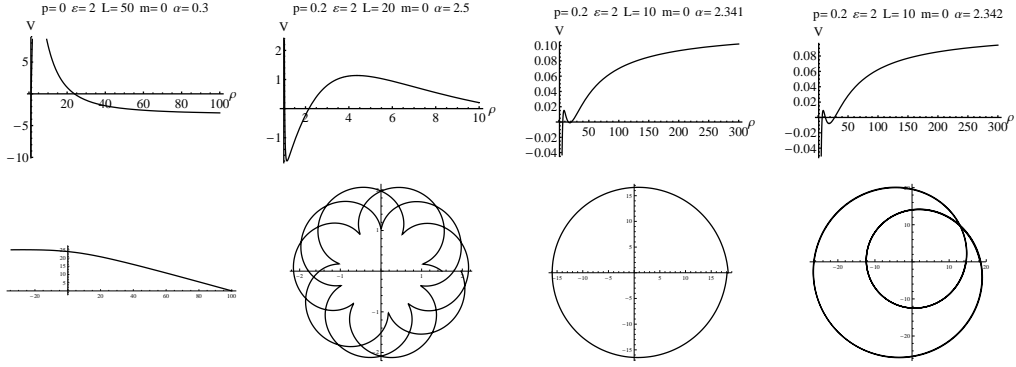


FIG. 8: The effective potential and lightlike geodesic orbits in naked singular spacetime with non-zero momentum along the z -direction.

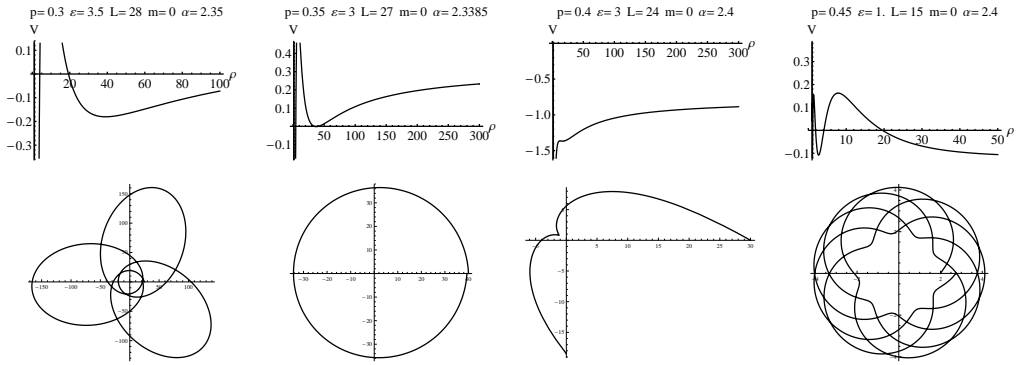


FIG. 9: The effective potential and lightlike geodesic orbits in black string spacetime with non-zero momentum along the z -direction.

The geodesic motion are obtained by solving the Hamilton-Jacobi equation to get the radial equation of motion. We analyzed the effective potential and showed that the geodesic motion may have many qualitatively different behaviors from those of spacetimes without “momentum charge”. Especially, any geodesic cannot arrive at $\rho = K$. In order to arrive there, a particle needs to follow non-geodesic trajectory. In addition, there are stable circular (or spiral) null geodesics which are absent for Schwarzschild geometry. The asymptotic region is allowed to particles with energy larger than $\sqrt{p_z^2 + m^2}$. The existence condition is crucially dependent on p_z .

We explicitly presented some geodesic trajectories numerically. In this work, we divided the timelike geodesics into two groups in terms of the value of momentum charge. The particles move in three different geometries, spacetime with the naked singularity, with the black string, or with the wormhole geometry. In the analysis of the geodesic motions, one can usually read off the behaviors of the radial motions from the shape of the effective potential. We also study the lightlike geodesics ($m = 0$) for non-zero momentum along the z -direction. There exist stable circular motions, elliptic motions, hyperbolic motions, and the unusual behavior of a light ray bouncing off the potential barrier.

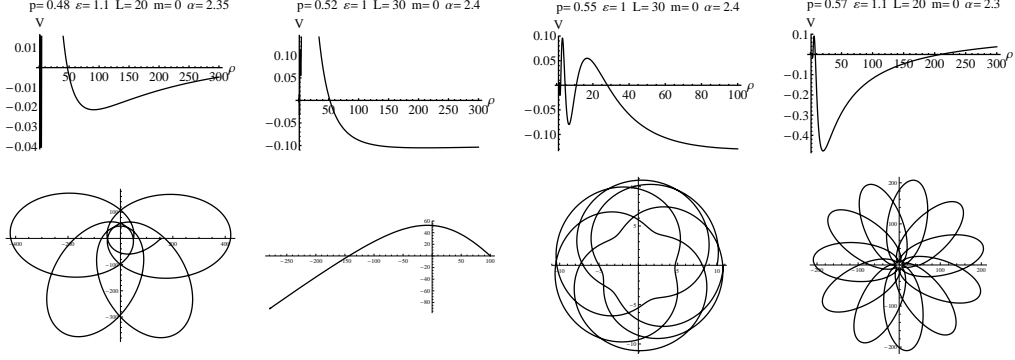


FIG. 10: The effective potential and lightlike geodesic orbits in wormhole geometry with non-zero momentum along the z -direction.

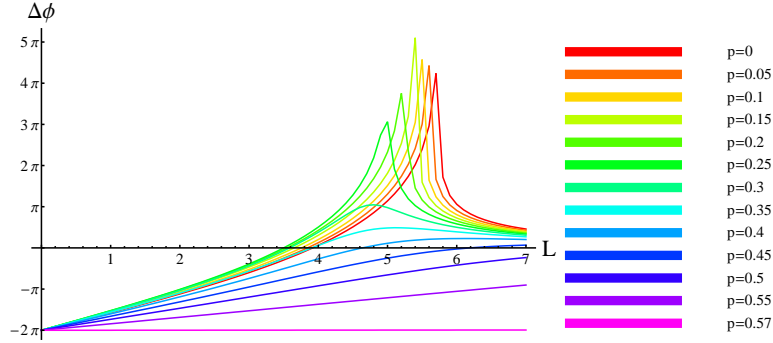


FIG. 11: A plot of the precession rate as a function of \mathbf{p} , where $m = 1$, $\mathcal{E} = 1$ and $\alpha = 0.1$.

In addition, we illustrated the orbit precession. The precession angle $\Delta\phi$ is -2π at $L = 0$ as expected. The numerical results show that it can be classified three groups in terms of the range of \mathbf{p} . In addition, it is indicated that we can identify the near horizon (or singularity) $\rho \simeq K$ property of the solution by analyzing the angular momentum dependence of the precession angle since the precession angle shows distinct features for each geometry. In the case of a naked singularity, as the angular momentum increases, the precession angle has a sharp peak which moves to the left as the “momentum charge” increases. In the case of a black string, it has a smooth peak which moves to the right. In the case of a wormhole geometry, there is no peak and the angle continually increases and approaches to zero.

Acknowledgments

We would like to thank Gungwon Kang and Hee Il Kim for their kind comments. This work was supported by the Korea Science and Engineering Foundation (KOSEF) grant funded by the Korea government(MEST) through the Center for Quantum Space-

time(CQuesT) of Sogang University with grant number R11-2005-021 and by the Korea Research Foundation Grant funded by the Korean Government(MOEHRD) KRF-2007-355-C00014(WL) and KRF-2008-314-C00063(H.-C. K.). BG is supported by the scholarship of Korea Science and Engineering Foundation (Scholarship Number:S2-2008-000-00800-1).

- [1] R. Gregory and R. Laflamme, Phys. Rev. D **37**, 305 (1988).
- [2] R. Gregory and R. Laflamme, Phys. Rev. Lett. **70**, 2837 (1993); T. Hirayama and G. Kang, Phys. Rev. D **64**, 064010 (2001).; S. S. Gubser and I. Mitra, High Energy Phys. **08**, 018 (2001).; M. W. Choptuik, L. Lehner, I. I. Olabarrieta, R. Petryk, F. Pretorius, H. Villegas, Phys. Rev. D **68**, 044001 (2003).; G. Kang and J. Lee, J. High Energy Phys. **03**, 039 (2004); T. Harmark and N. Obers, [hep-th/0503020]; H. Kudoh, Phys. Rev. D **73**, 104034 (2006); Y. Brihaye, T. Delsate, and E. Radu, Phys. Lett. B **662**, 264 (2008).
- [3] G. T. Horowitz and K. Maeda, Phys. Rev. Lett. **87**, 131301 (2001); S. S. Gubser, Class. Quant. Grav. **19**, 4825 (2002).
- [4] D. Kramer, Acta Phys. Polon. B **2**, 807 (1971); J. Gross and M. M. Perry, Nucl. Phys. **B226**, 29 (1983); A. Davidson and D. A. Owen, Phys. Lett. B **155**, 247 (1985).
- [5] A. Chodos and S. Detweiler, Gen. Relativ. Gravit. **14** 879, (1982).
- [6] C. H. Lee, Phys. Rev. D **74**, 104016 (2006).
- [7] J. Traschen and D. Fox, Class. Quant. Grav. **21**, 289 (2004) [arXiv:gr-qc/0103106].
- [8] I. Cho, G. Kang, S. P. Kim and C. H. Lee; J. Korean Phys. Soc. **53**, 1089 (2008); G. Kang, H.-C. Kim, and J. Lee, Phys. Rev. D **79**, 124030 (2009).
- [9] S. Yun, Mod. Phys. Lett. A **25**, 159 (2010).
- [10] H.-C. Kim and J. Lee, Phys. Rev. D **77**, 024012 (2008).
- [11] C. W. Misner, K. S. Thorne, and J. A. Wheeler, *Gravitation* (Freeman, San Francisco, 1973).
- [12] T. Matos and N. Breton, Gen. Relativ. Gravit. **26** 827, (1994).
- [13] B. Gwak, B.-H. Lee, and W. Lee, J. Korean Phys. Soc. **54**, 2202 (2009).
- [14] J. Lee and H.-C. Kim, Mod. Phys. Lett. A **22**, 2439 (2007).
- [15] J. Lee and H.-C. Kim, Mod. Phys. Lett. A **23**, 305 (2008).
- [16] H. Y. Liu, P. Wesson and J. Poince de Leon, J. Math. Phys. **34**, 4070 (1993).
- [17] A. Billyard and P. S. Wesson, Phys. Rev. D **53**, 731 (1996).
- [18] K. S. Virbhadra and G. F. L. Ellis, Phys. Rev. D **65**, 103004 (2002).
- [19] K. S. Virbhadra, Phys. Rev. D **79**, 083004 (2009).